9th ANKARA INTERNATIONAL AEROSPACE CONFERENCE AIAC-2017-121
20-22 September 2017 - METU, Ankara TURKEY

EFFECT OF WING DEFORMATION ON AERODYNAMIC LOADS AT SUPERSONIC SPEEDS

Emir Ozkokdemir[1]
Roketsan Missile Inc.
Ankara, Turkey

Dilek Funda Kurtulus[2]
Middle East Technical University
Ankara, Turkey

ABSTRACT

Aerodynamic performance of wings is directly related to the flow characteristics and the wing geometry. The change in the wing geometry by external loads such as the temperature gradient formed by aerodynamic heating and the pressure distribution on wing surfaces affect the flow characteristics around the wing. In addition, the change in the flow characteristics affects the structural and the thermal loading on the wing. Therefore, aerodynamic performance for undeformed wing has not the same performance as the deformed wing configuration. In the current study, a wing based on NACA65-009 airfoil is selected as a test case at zero angle of attack. Two and three dimensional flow characteristics are investigated. Effect of the three dimensional deformation on aerodynamic performance is presented.

INTRODUCTION

A flight at high speeds and high altitudes introduces many new problems to the designer. One of the important problems is caused by the aerodynamic heating generated on wing at high velocities. At supersonic and hypersonic flight regimes, the airflow around the wing is heated due to the decrease in the flow kinetic energy near the wall. At the same time, the wing body is heated by the skin friction within the boundary layer on the wing surface. Adiabatic wall temperatures under these conditions can exceed strength limitations of structural materials commonly used in the wings or fins. This is the most common problem that forces designers to find better aerodynamic wing design.

The aerodynamic coefficients are directly related to the wing geometry. The change in the wing geometry by external loads due to the temperature gradient is formed by aerodynamic heating and the pressure distribution on the wing surface. The aerodynamic performance for undeformed wing is not the same as for deformed wing. Therefore, the deformation on the wing must be taken into account in the performance calculations. The aim of this study is to

[1] Specialist Engineer in Structural, Thermal, Dynamic Analysis and Test Department, Email: emir.ozkokdemir@roketsan.com.tr
[2] Assoc. Prof. Dr. in a Aerospace Engineering Department, Email: funda.kurtulus@ae.metu.edu.tr

investigate the change of the aerodynamic performance by wing deformation created by the thermal and structural loadings.
In the previous studies of the authors, the flow simulations of various airfoils at low Reynolds number are investigated [Kurtulus, 2005; 2015; 2016]. Structural integrity and flow characteristics of airfoils at supersonic flow regime are investigated [Kayabasi et al., 2012; Ozkokdemir et al., 2016; Aslan et al., 2016].
Drag measurements of NACA65-009 and circular arc wing on missile body are carried on a study [Alexander et al., 1947]. In addition, the effect of sweep angle on drag characteristics is investigated at different aspect ratios in this study. Flight tests have been conducted at supersonic speed from 0.85 to 1.22 Mach. In this study results for NACA 65-009 wing are selected as the validation case.
The supersonic channel airfoil design technique significantly reduces the drag in high speed flows over diamond shaped airfoils [Giles et al., 2008]. The model used for the demonstration of the effect of this technique is NACA66-206. A three dimensional wing is designed with the determined slot geometry. Results showed an increase in the lift-to-drag ratio for airfoils at Mach 2.5 showing a benefit of 17.2% at 6° angle of attack and a sharp channel leading edge. An overall increase in the lift-to-drag ratio of 9% is achieved at Mach 2.5 and 6° angle of attack.
In another study [Borovoy et al.,1993], the flow and heat transfer on the fins attached to the side wing edges on the tip fins and on the fins located at a distance from the side wing edges are investigated. The tests are carried out at 5 and 8 Mach numbers and Reynolds numbers ranging from 0.6 $x10^6$ to $1.1x10^6$. The heat flux is measured by thermal sensitive coatings. It is found that the heat transfer coefficient on its windward side rises because of the increase of the wing angle of attack and the heat transfer coefficient varies weakly outside of the interference zone. The heat transfer coefficient at the leeward surface of the fin reduced in the level to be ignored by the increase in the fin angle.

METHOD

In the current study, the deformation of the wing exposed to the external loads is obtained and the effect of deformation on the aerodynamic performance such as drag and lift is investigated. The deformation on the wing is obtained by a series of conjugate computational fluid dynamic simulations and sequentially coupled (thermal and structural) finite element simulations. Computational fluid dynamic simulations are used to obtain external loads on the wing and sequentially coupled finite element simulations are used to obtain the deformation on the wing. Flow and structural simulations are carried on Ansys Fluent and Abaqus Standard respectively.

Governing Equations and Geometry

The unsteady, viscous and three dimensional conservation equations for compressible fluid are given between Eq.(1) and Eq.(5).

$$\frac{\partial \rho}{\partial t} + \mathrm{div}(\rho \mathbf{u}) = \mathbf{0} \tag{1}$$

$$\frac{\partial(\rho u)}{\partial t} + \mathrm{div}(\rho u \mathbf{u}) = -\frac{\partial p}{\partial x} + \mathrm{div}(\mu\ \mathrm{grad}\ u) + S_{M_x} \tag{2}$$

$$\frac{\partial(\rho v)}{\partial t} + \mathrm{div}(\rho v \mathbf{u}) = -\frac{\partial p}{\partial y} + \mathrm{div}(\mu\ \mathrm{grad}\ v) + S_{M_y} \tag{3}$$

$$\frac{\partial(\rho w)}{\partial t} + \mathrm{div}(\rho w \mathbf{u}) = -\frac{\partial p}{\partial z} + \mathrm{div}(\mu\ \mathrm{grad}\ w) + S_{M_z} \tag{4}$$

$$\frac{\partial(\rho i)}{\partial t} + \mathrm{div}(\rho i \mathbf{u}) = -p\ \mathrm{div}\ \mathbf{u} + \mathrm{div}(k\ \mathrm{grad}\ T) + \Phi + S_i \tag{5}$$

where S_M is momentum source, Φ is dissipation function, **u** is the velocity vector, u,v,w are the velocity components in x,y,z directions , ρ is the fluid density, p is the pressure, μ is the dynamic viscosity and i is internal energy of the fluid. Ansys Fluent implements the finite-volume method to solve conservation equations. The pressure-velocity coupling is done by means of the SIMPLE-type fully implicit algorithm.

Aerodynamic performance of a wing is determined from aerodynamic coefficients such as the drag coefficient (C_D) and the lift coefficient (C_L) given by Eq. (6) and Eq. (7), respectively.

$$C_D = \frac{D}{\frac{1}{2}\rho U_\infty^2 S} \tag{6}$$

$$C_L = \frac{L}{\frac{1}{2}\rho U_\infty^2 S} \tag{7}$$

where D is drag, L is lift, ρ is the density, U_∞ is the free stream velocity, S is the planform wing area.

For 2D simulations, the lift and drag coefficients are given by Eq. 7 and Eq. 8, respectively.

$$C_d = \frac{D}{\frac{1}{2}\rho U_\infty^2 c} \tag{7}$$

$$C_l = \frac{L}{\frac{1}{2}\rho U_\infty^2 c} \tag{8}$$

where D' is drag per unit span, L' is lift per unit span, ρ is the density, U_∞ is the free stream velocity, c is the chord length of the airfoil.

A zero angle of attack wing based on 9.647 in (245mm) chord with NACA 65-009 [Abbott, 1945] airfoil is used as a test case given in Figure 1. Two dimensional and three dimensional calculations have been done and the results are compared with the flight test data [Alexander et al., 1947]. Two dimensional cases are used for the grid refinement study and the method validation. On the other hand, the effect of deformation on aerodynamic coefficients is investigated in three dimensional cases.

Grid Refinement Study and Simulation Models

Detailed grid refinement studies are performed by using three different meshes. Structural elements are used at the boundary layer and unstructured elements are used outside of the boundary layer. Total numbers of elements used for the grid refinement study are presented in Table 1. The first cell spacing of the boundary layer is about 3.5×10^{-6}c for all mesh levels. The grid for all mesh levels are shown in Figure 2. The grid is also generated inside of the airfoil in order to perform conjugate heat transfer. The pressure far field inlet boundary condition is used at inlet sections of the outer domain and pressure outlet was used at the outer regions.

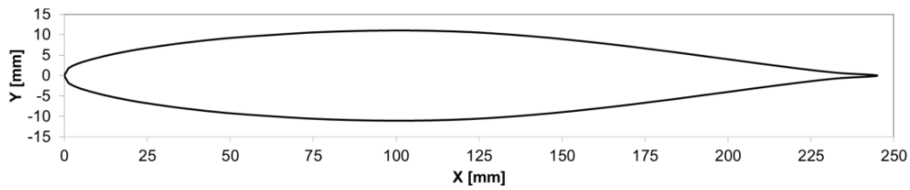

Figure 1: NACA 65-009 Airfoil

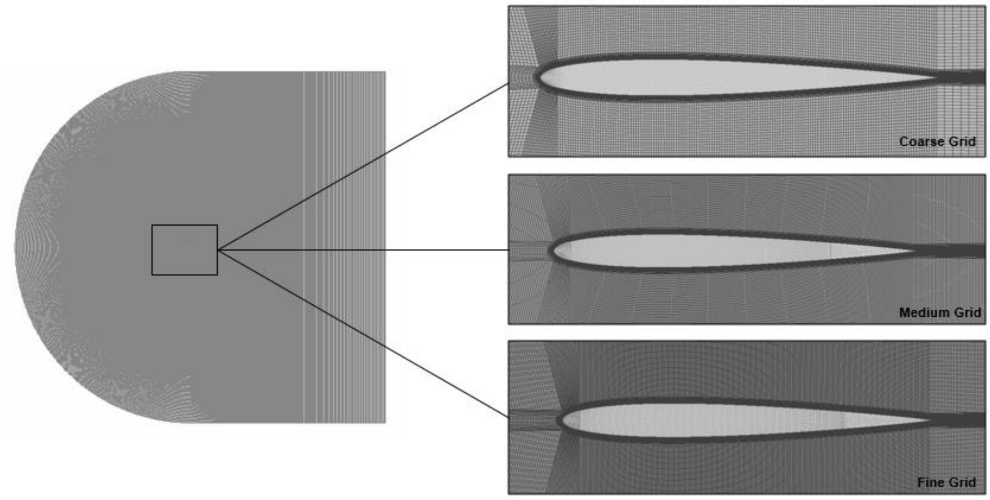

Figure 2: 2D Flow Domain for CFD Simulation

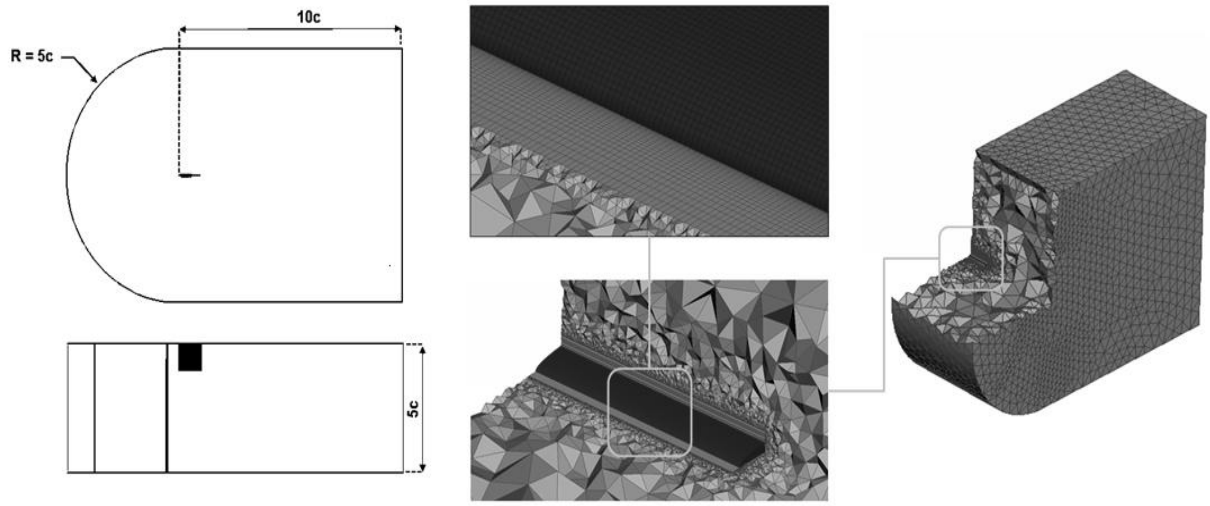

Figure 3: 3D Flow Domain for CFD Simulation

Computational fluid dynamic simulations are carried out for the two dimensional NACA65-009 airfoil. In order to investigate the 3D wing tip effect, the three dimensional NACA65-009 wing which has the same aspect ratio as the flight test case [Alexander et al., 1947] is also simulated. Flow domain of the clean wing model is shown in Figure 3. Number of elements for the clean wing model is 11.2 million and this is a limit for the current hardware that we are using for the simulations; therefore, three dimensional flow simulations are performed at this mesh level. The grid of the clean wing model includes structural elements for the boundary layer and unstructured elements for outside of the boundary layer.

The results of flow simulations are compared with the flight test data [Alexander et al., 1947]. In the flight test, a missile body equipped with NACA65-009 wing has been tested at different Mach numbers ranging from 0.85 to 1.22. The drag coefficient obtained from the flight test at 1.19 Mach for clean wing configuration is given in Figure 4. The altitude of the flight test data was not available. In the current simulations, the flow properties are taken at sea level conditions. The difference in the altitude between the test conditions and simulations results in the difference in C_D calculations.

Table 1: Grid Refinement Study

Mesh Level	# of elements
Coarse mesh (2D)	746 936
Medium mesh (2D)	1 685 730
Fine mesh (2D)	2 326 766
Clean Wing Mesh (3D)	11 197 318

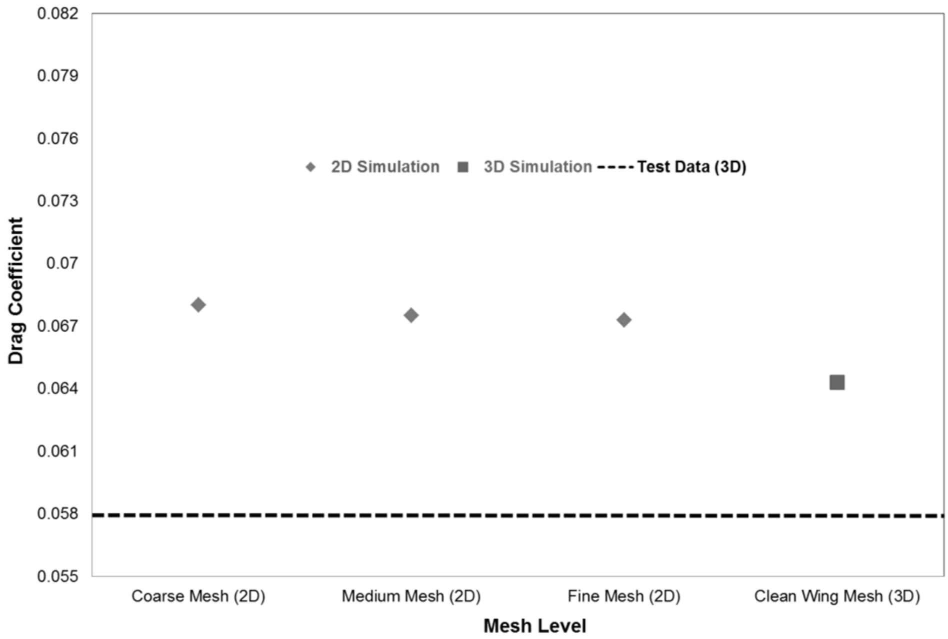

Figure 4: Comparison of Drag Coefficient for Different Meshes (M=1.19)

For three dimensional simulations, the procedure of the method is shown in Figure 5. Flow and structural problems are solved sequentially. The external loads (thermal loads and pressure) exerted on the wing are calculated and then used in the structural part for the deformation calculations. The finite element model used in the structural part is shown in Figure 6. The wing and the missile body shown in Figure 6 are made of Aluminum 2000 series and the material properties are given in Table 2.

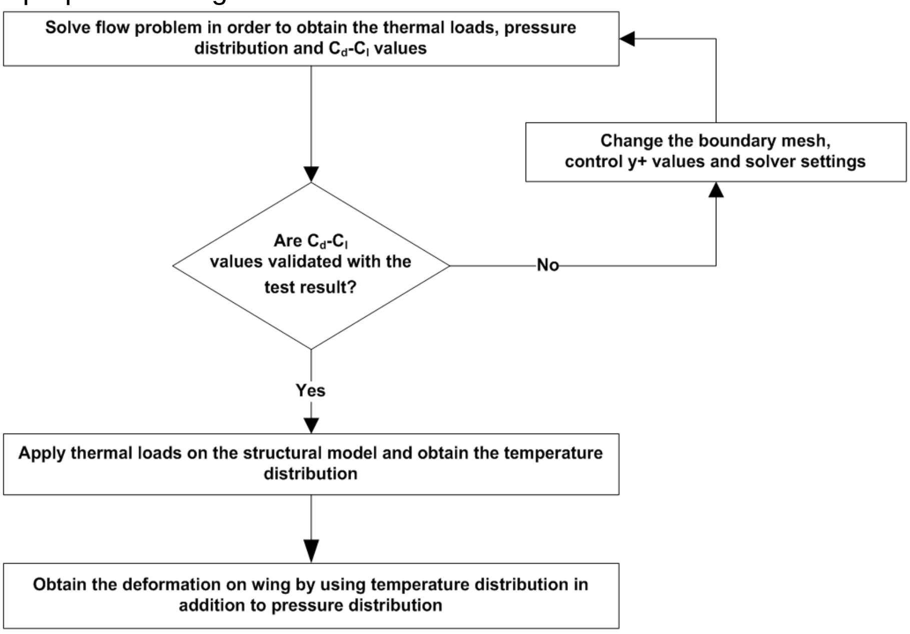

Figure 5: Procedure of the Method

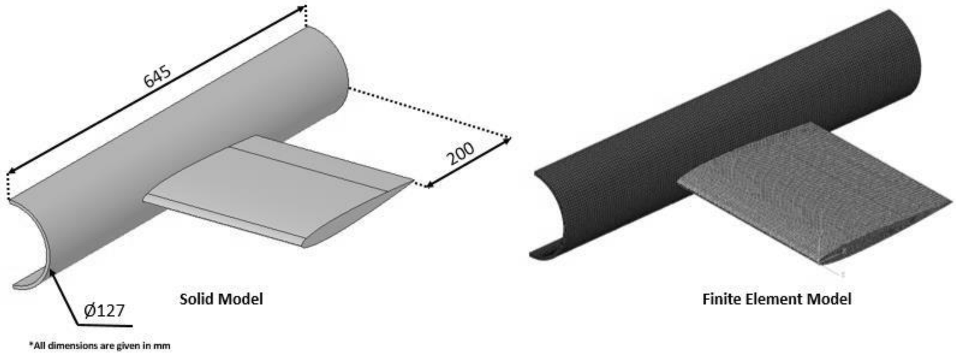

Figure 6: Finite Element Model

Table 2: Material Properties of Aluminum 2000 series

Property	Value
Density (kg/m³)	2770
Young Modulus (MPa)	72814
Poisson Ratio	0.33
Expansion (1/°C)	$2.2x10^{-5}$
Conductivity (W/m.K)	120
Specific Heat (J/kg.K)	900

RESULTS

Two Dimensional Numerical Simulations

The two dimensional flow simulations are performed at medium mesh for different free stream velocities. Static pressure, static temperature and Mach number contours are presented in Figure 7. The external loads (static pressure, static temperature and heat transfer coefficient) exerted on the wing surfaces are demonstrated in Figure 8.

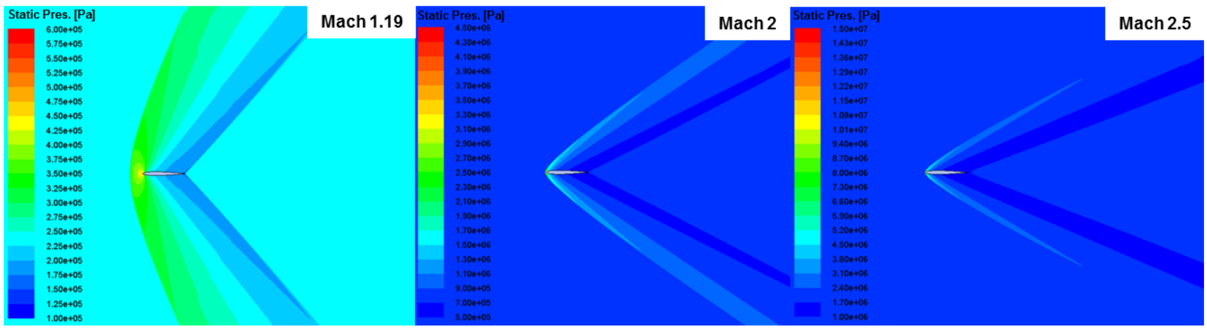

(a)

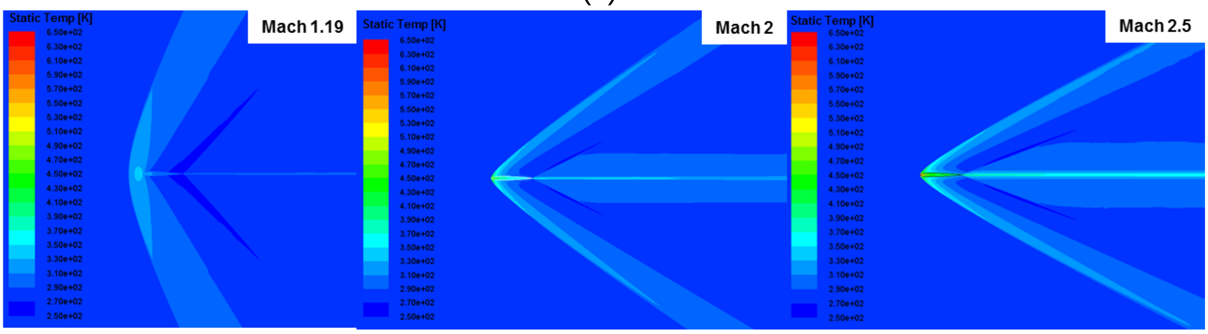

(b)

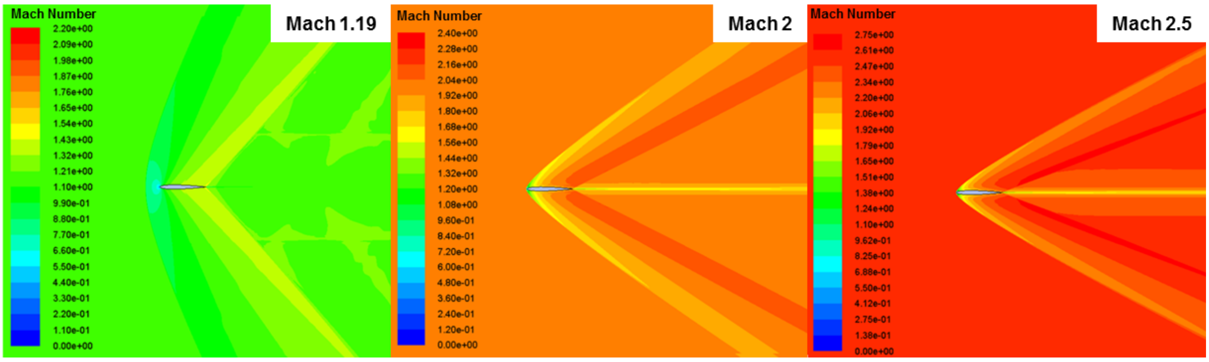

(c)

Figure 7: CFD Problem Solution (2D) over the Flow Domain (a) Static Pressure (b) Static Temperature (c) Mach Number Contours at Different Free Stream Mach Numbers

It is seen in figures that the static temperature and the static pressure decrease from the leading edge to the trailing edge. Approximately 80% of the thermal loading acts on the wing surfaces is placed near leading edge. An increase in the flow speed at a point on wing surface generally causes an increase in the external loads calculated at the same point but the heat transfer coefficient has a random behavior near leading and trailing edge. The change of drag coefficient with the flow speed is presented in Figure 9.

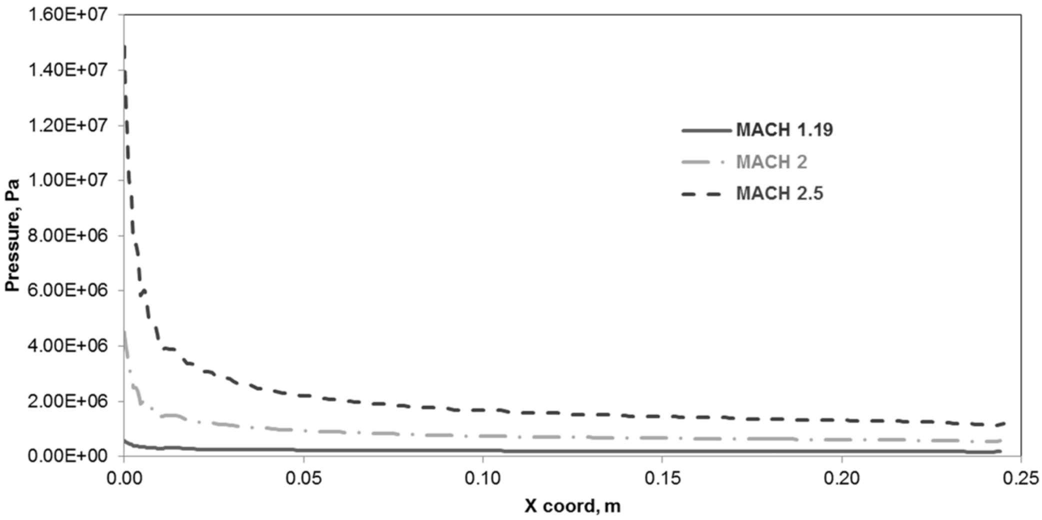

(a)

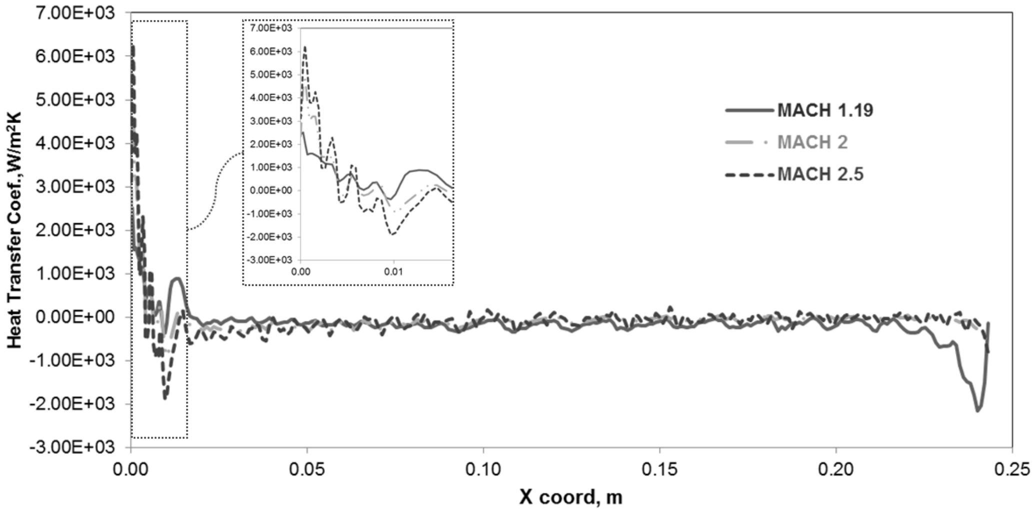

(b)

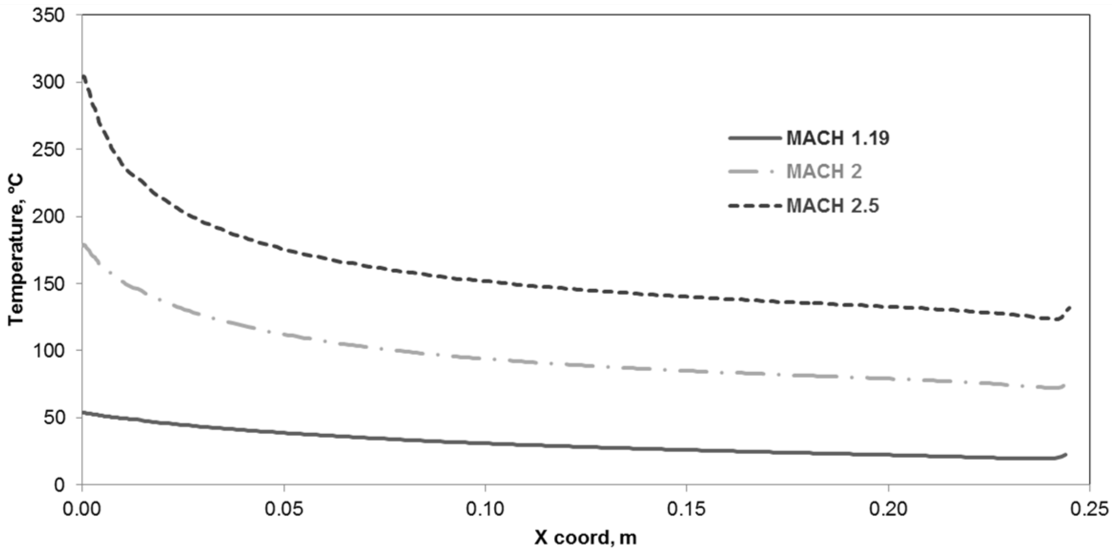

(c)

Figure 8: External Loads on the Wing Surfaces (a) Static Pressure (b) Heat Transfer Coefficient (c) Static Temperature

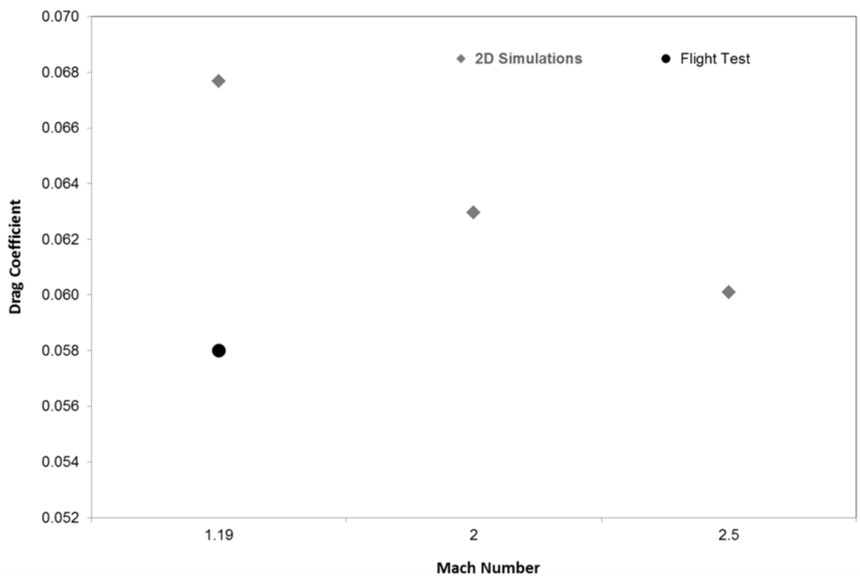

Figure 9: Drag Coefficient for Different Mach Numbers (2D)

Three Dimensional Numerical Simulations

<u>Three Dimensional Computational Fluid Dynamics Simulations</u>

In the first part of the three dimensional simulations, the flow problem has been solved for three different Mach numbers at zero angle of attack. Comparisons of static pressure, static temperature and Mach number contours are demonstrated in Figure 10.

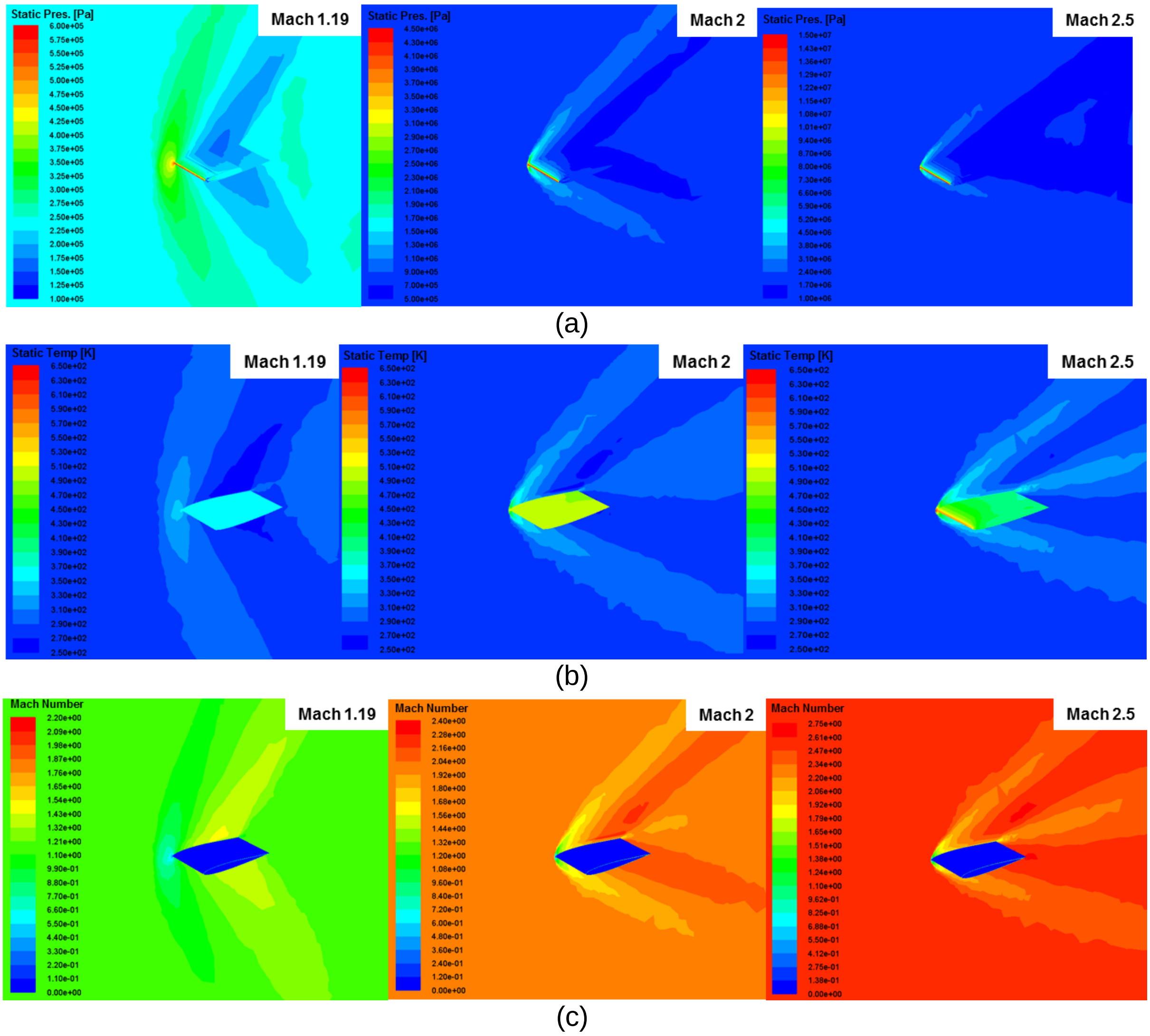

Figure 10: CFD Problem Solution (3D) over the Flow Domain (a) Static Pressure (b) Static Temperature (c) Mach Number Contour at Different Free Stream Mach Numbers

Increase in flow speeds causes an increase in the amount of energy transformation from the kinetic energy to the heat energy. Also a smaller shock wave distance at leading edge is formed by increasing flow speed. Therefore, the temperature values near the leading edge are increased more than other part of the wing.

The drag coefficient variation with the free stream Mach number for 3D configuration is presented in Figure 11. As shown in Figure 11, the drag coefficient is decreasing with the free stream Mach number.

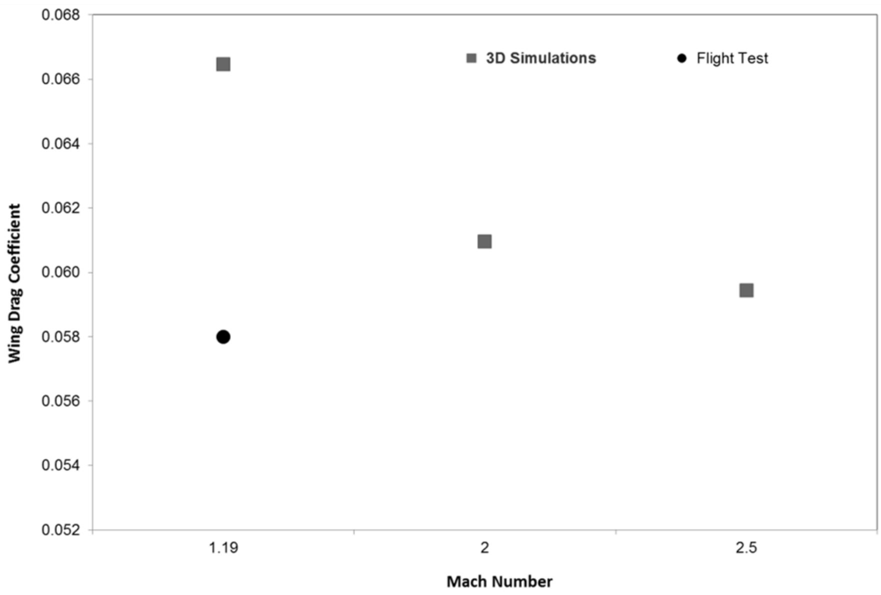

Figure 11: Drag Coefficient for Different Free Stream Mach Numbers (3D)

<u>Three Dimensional Finite Element Simulations</u>

In the second part of the three dimensional numerical simulations, the external loads calculated from the first part are used as inputs in order to obtain the deformation rates on the wing as given in Figure 6.
The deformation rates on the wing/body configuration calculated by using the external loads obtained from free stream Mach numbers of 1.19 and 2 are relatively small and considered to be negligible. Deformation rates are presented for free stream Mach number of 2.5 are presented in Figure 12. The maximum wing displacement is observed to be 3.85 mm.

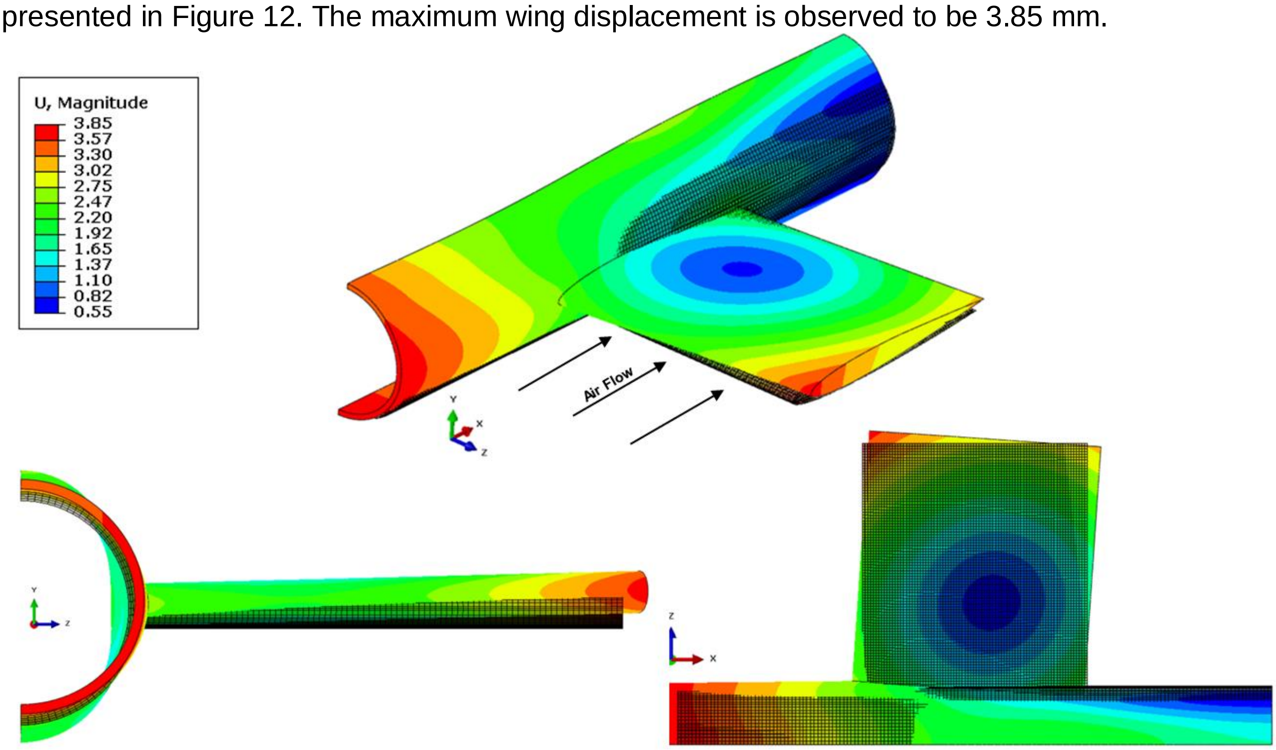

Figure 12: Deformation on Wing Body for 2.5 Mach (mm)

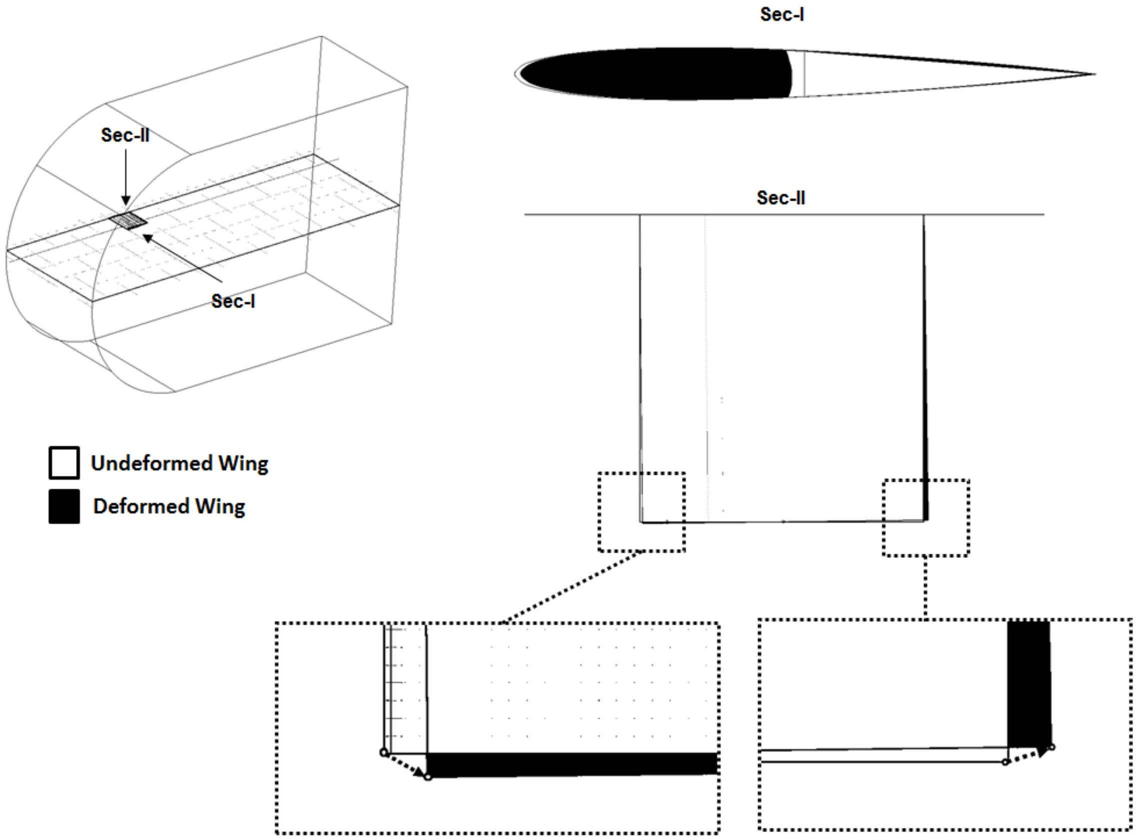

Figure 13: Deformed and Undeformed Wing CFD Model for 2.5 Mach

The flow simulation for 2.5 Mach is performed with the deformed wing body and wing drag coefficient is recalculated. CFD model of the deformed wing body is represented in Figure 13. The CFD results of deformed wing given in Figure 14 are compared to the results of undeformed wing. The comparison of the effect of deformation on the drag coefficient is demonstrated in Table 3. As shown in Table 3, the wing drag coefficient is increased with deformation by 5.1 percent.

Table 3: Wing Drag Coefficient (C_D) for Deformed and Undeformed Wing

	Undeformed Wing	**Deformed Wing**	**Percent Change [%]**
C_D	0.059	0.062	5.1

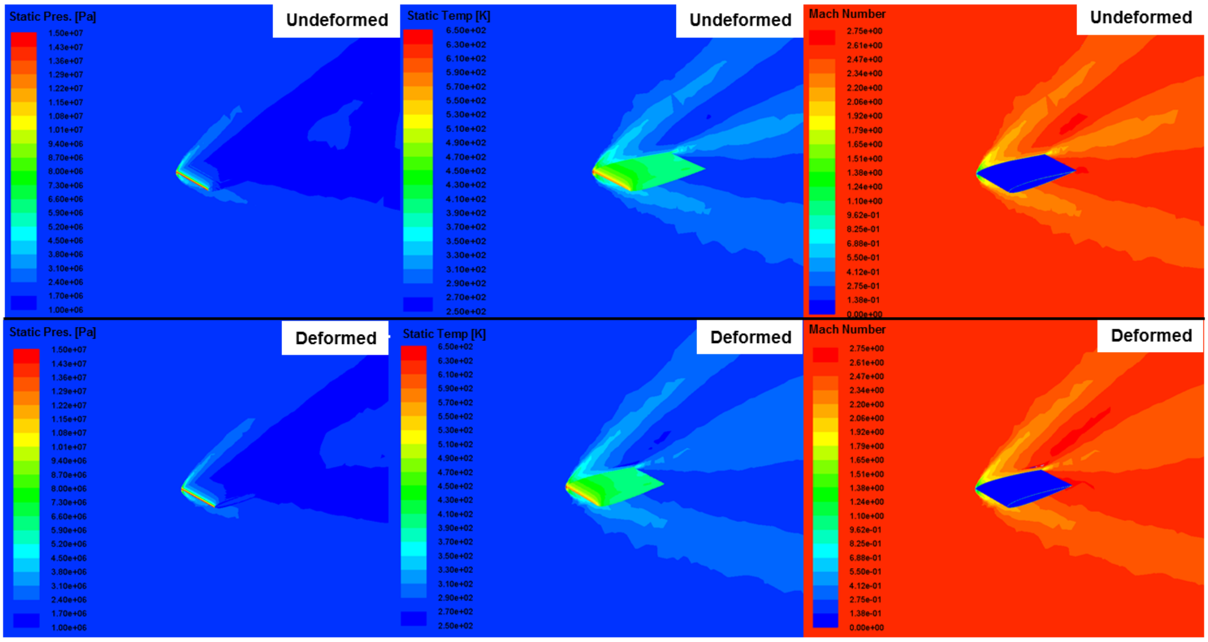

(a) (b) (c)

Figure 14: Comparison of (a) Static Pressure (b) Static Temperature (c) Mach Number Contours of Undeformed and Deformed Wings (M=2.5)

CONCLUSION

A methodology is developed to obtain the effect of wing deformation exposed to high temperature on aerodynamic performance. Two dimensional simulations are performed for method validations and grid refinement. The results of CFD part are compared with the test data [Alexander et al., 1947].

The deformation of wing body is investigated in three dimensional numerical simulations. The deformed wing geometry is obtained according to the results of the undeformed wing finite element simulations. The CFD part of the numerical simulations is repeated with the deformed wing to obtain the effect of the wing deformation on the aerodynamic performance.

In the current simulations, the flow properties are taken at sea level conditions. The difference in the altitude between the test conditions and simulations results in the difference in C_D calculations.

For the future work, the effect of the missile body on the flow characteristics will be investigated. More accurate results are aimed to be obtained.

References

Abbott I.H., Von Doenhoff A.E. (1945), *Summary of Airfoil Data*, NACA Report:824, 1945

Alexander S.R. (1947), *Drag Measurements of Symmetrical Circular-arc and NACA 65-009 Rectangular Airfoils Having an Aspect Ratio of 2.7 as Determined by Flight Tests at Supersonic Speeds*, NACA Research Memorandum Doc. No:L6J14, 1947

Alexander S.R. Katz E. (1947), *Drag Characteristics of Rectangular and Swept-Back NACA 65-009 Airfoils Having Aspect Ratios of 1.5 and 2.7 as Determined by Flight Tests at Supersonic Speeds*, NACA Research Memorandum, No:L6J16, 1947

Aslan M. G., Kurtulus D.F. (2016), *Füze Kanadının Ses Üstü Uçuş Koşulundaki Aeroelastik Analizi*, VI. Ulusal Havacılık ve Uzay Konferansı, Kocaeli Üniversitesi, Kocaeli, 2016

Borovoy V.Y., Kubyshina T.V. (1993), *Hypersonic Heat Transfer on the Upper Wing Surface Fins*, AIAA/DGLR 5th International Aerospace Planes and Hypersonic Technologies Conference, 1993

Giles D.M., Marshall D.D. (2008), *Aerodynamic Performance Enhancement of a NACA 66-206 Airfoil Using Supersonic Channel Airfoil Design*, AIAA 46th AIAA Aerospace Sciences Meeting and Exhibit, 2008

Kayabaşı İ., Akgül A., Kurtuluş D.F. (2012), *NACA0012 Kanat Profili için Sinusoidal Yunuslama Hareketinin Hesaplamalı Akışkanlar Dinamiği ile Modellenmesi*, IV. Ulusal Havacılık ve Uzay Konferansı, 2012

Kurtulus D.F. (2005), *Numerical and Experimental Analysis of Flapping Motion in Hover. Application to Micro Air Vehicles*, Joint Ph.D thesis Poitiers University/ENSMA (Poitiers-France) and METU (Ankara-Turkey), 2005

Kurtulus D.F. (2015), *On the Unsteady Behavior of the Flow Around NACA 0012 Airfoil with Steady External Conditions at Re=1000*, International Journal of Micro Air Vehicles, Vol 7, No 3, pp 301-326, 2015

Kurtulus D.F. (2016), *On the Wake Pattern of Symmetric Airfoils for Different Incidence Angles at Re=1000*, International Journal of Micro Air Vehicles, Vol 8, No:2, 2016

Ozkokdemir E., Kurtulus D.F. (2016), *Investigation of the Mechanical Integrity of Wings/Fins under Thermal Loading*, Ninth International Conference on Computational Fluid Dynamics, ICCFD9, Istanbul, 2016